Channel Variability in Human Body Communication with External Objects in Body Resonance Region

Qi Huang, *Student Member, IEEE*, Samyadip Sarkar, *Student Member, IEEE*, Shreyas Sen, *Senior Member, IEEE*

***Abstract*—The channel variability of human body communication (HBC) in Electro-Quasistatic (EQS) region and the influence of the parasitic paths by external objects and inter-body coupling have been widely explored. However, channel variability of HBC in the body resonance (BR) region is hardly studied. In the BR region, the wavelength is comparable to the dimension of the human body which starts to resonate and act as an antenna. Electromagnetic (EM) wave patterns are generated from the transmitter dipole and formed on the human body. The external objects causing some parasitic paths influence the patterns and the channel gain. This paper explores the influence of external objects on the HBC channel gain in the BR region for the first time. Firstly, the relevant EM theories and corresponding simulation setup and results are introduced. Following that, the experiment setup and results are described and analyzed. The results show that putting the arms on the table can lead to a notch frequency shift by 77∼100 MHz and channel gain change by -17∼20 dB depending on different angles and frequencies. The channel gain variation before the notch is small, enabling stable high-speed communication.**

***Index Terms*—Human Body Communication (HBC), Channel gain measurement, External object, Body resonance region, Electromagnetics**

I. Introduction

Over the last few decades, HBC, as an alternative to radio frequency (RF) communication to interconnect the biosensors throughout the body, has attracted much scholarly attention and gained much popularity. The HBC in the BR regime, compared with the EQS-HBC, has a large bandwidth (BW) that can support applications with high data rates, such as audio and video streaming, endoscope capsules, gaming consoles, and so on. The channel feature of EQS HBC has been comprehensively explored from all kinds of aspects over the past few decades but the studies on the channel characteristics of the BR HBC are still limited. Moreover, the surrounding factors, including electric appliances, mobile devices, surrounding objects, ambient sources, and wearables, may influence the channel characteristics, as shown in Fig.1 (a). Particularly, the influence of external objects on the BR HBC channel gain has not been explored.

Ž. Lucev et al. [1] explored the channel gain of capacitive HBC using a benchtop ground-connected vector network analyzer (VNA) with and without a balun. The frequency range is from 100 kHz to 100 MHz. However, the improper ground isolation leads to over-optimized channel gain. S. Maity et al. [2] studied the influence of different termination impedances on the channel gain of the EQS HBC with self-designed wearable devices from 10 kHz to 1 MHz. High impedance and capacitive terminations are preferred instead of 50 Ω at the receiver side to improve the channel gain and help broadband communications. D. Yang et al. [3] explored the channel variation with different postures, environmental conditions, and body locations at 415 kHz. Leakage measurements are also implemented at the same frequency to show the maximum distance from the body where the signal can still be detected. S. Sarkar [4] explored the channel gain of EQS HBC with a structure (surrounding conducting object) to interact with the human body. Measurements with different RX configurations (floating-grounded and ground-connected) and different structure positions are implemented. It is found that the human between conducting structures can boost the received voltage by ∼8 dB with wearable devices and ∼18 dB with a grounded receiver. J. Park et al. [5] compared the channel gain with different measurement setups, including VNA without and with a balun, spectrum analyzer (SA) with and without balun, as

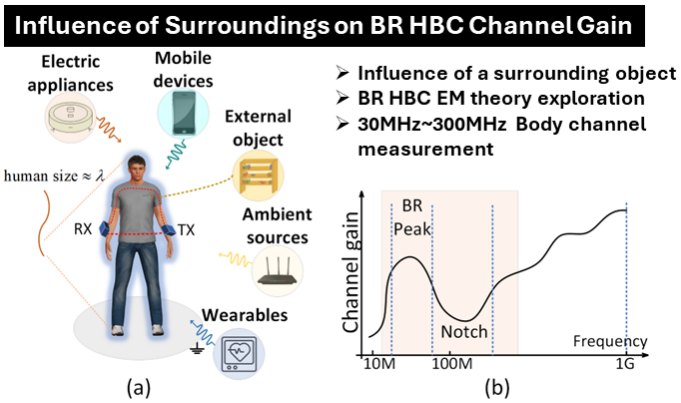

	Wearable TRx	Frequency	EQS/BR	External object
Z. Lucev et al.	No	100kHz~100MHz	EQS	No
S. Maity et al.	Yes	10kHz~1MHz	EQS	No
S. Sarkar et al.	Yes	1MHz	EQS	Yes
D. Yang et al.	Yes	415kHz	EQS	Yes
P. Mercier et al.	Yes	20MHz~150MHz	BR	No
S. Avlani et al.	Yes	100kHz~1GHz	BR	No

(c)

Fig. 1: (a) Influence of surrounding objects on BR HBC channel gain. At BR frequencies, the human size is comparable to the wavelength. (b) The trend of channel gain beyond EQS region. The red square shows the frequency range (30 MHz ∼ 300 MHz) of this work. (c) Comparison of explorations on HBC channel characteristics [1]–[6]

Qi Huang, Samyadip Sarkar, and Shreyas Sen are with the School of Electrical and Computer Engineering, Purdue University, USA {huan2065, sarkar46, shreyas}@purdue.edu

well as wearable prototypes at 50 Ω receiver impedance. The frequency range of the measurement is 20 MHz to 150 MHz. The impedance matching work is applied to maximize the received power. S. Avlani et al. [6] explored the channel gain from 100 kHz till 1 GHz at 50 Ω receiver impedance and 1 MΩ || 2.1 pF. Similarly, high impedance termination leads to a significantly lower path loss and this difference decreases with the increasing of the frequency. Moreover, the body resonance peak can be apparently observed. A summary of the above-mentioned papers is shown in Fig. 1 (c).

In the BR frequencies, the wavelength has the same magnitude as the human body size so that the human body starts to resonate as a monopole antenna [7]. The general trend of the channel gain of the BR HBC is shown in Fig. 1 (b). At a lower frequency with near-field, the electrostatic dipole operates. With the frequency going higher, the far-field operation dominates. The BR peak is caused when the dipole signal for the first time resonates the human body and the notch happens when the first far-field notch pattern arrives at the receiver side. Then the channel gain increases with sinusoidal fluctuations depending on the wavelength. This paper for the first time explores the influence of a table as the external object on the channel characteristics of BR HBC. The rest of the paper is organized as follows. Section II introduces the High-frequency Structure Simulator (HFSS) simulation setup and results. Section III describes the experiment setup, calibration process as well as experiment procedures. Section IV describes and analyzes the experiment results. Section V contains the conclusion.

II. Simulation Setup and Results

To study the influence of a table as an external object on the channel characteristics of the BR HBC, simulations are first carried out with HFSS, a finite element method (FEM)-based EM solver.

A. Simulation setup

The simplified model with the cross cylinders with the human tissue properties (conductive and dielectric) from Gabriel et al. [8] is used for the simulation. Compared with the complex human model - VHP Female v2.2 from Neva Electromagnetics [9], it has identical electric and magnetic distributions inside the human body, and model complexity is greatly reduced for faster simulations with the same accuracy [10]. Fig. 2 (a) shows the overall simulation setup with the table. The human torso is 180 cm tall. The radii of the skin and muscle are 4 mm and 13.6 mm. The arms are placed on the surface of the table with a rotation angle θ. The table surface is made of plywood with an ϵ of 8.13, and the table legs are made of steel metal. Other parameters are marked in the Fig. 2 (a). The transmitter and the receiver are placed on the two arms on the table. Each of them comprises a signal electrode and a ground electrode. Three rotation angles θ are selected, 50, 65, and 80 degrees. There has not been a clear boundary between EQS and BR frequency regions, the frequency sweeping range we select is from 30 MHz to 300 MHz which contains the BR peak and notch regions, as shown by the reddish box in Fig. 1 (b).

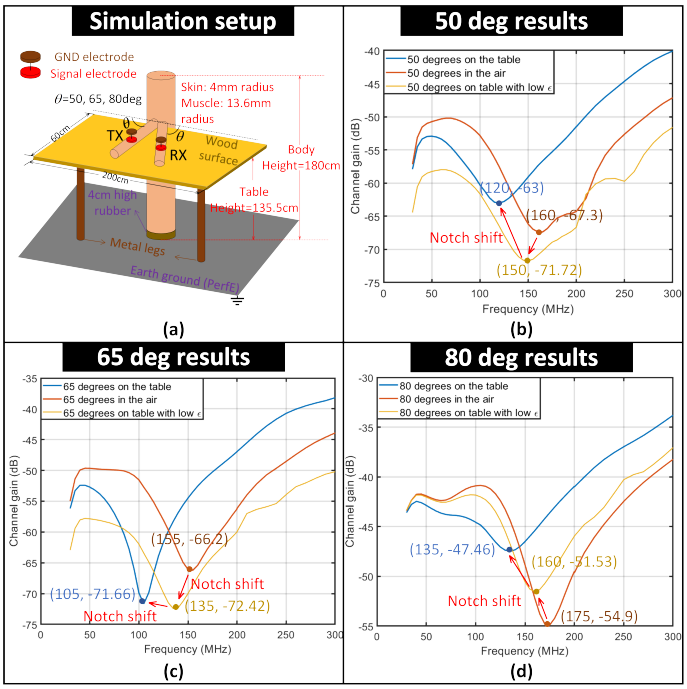

Fig. 2: Simulation setup and results. (a) Simulation setup. (b) (c) (d) Simulation results. The blue line shows the results when the arms are put on the table with $\epsilon_r = 8.13$. The red line shows the results when the arms are in the air. The yellow line shows the results when the arms are put on the table with $\epsilon_r = 2$

B. Simulation results

The simulation results are shown in Figs. 2 (b), (c), (d). The red curve shows the results in the air while the blue one shows the results when putting the arms on the table. As can be observed from the figures, the notch and the trend of the whole curve shift leftward. This is caused by the participation of a dielectric with a higher relative permittivity ϵ_r. According to $\lambda = \frac{\lambda_0}{\sqrt{\epsilon_r \mu_r}}$, where the λ_0 is the wavelength of the electromagnetic wave in the vacuum space, ϵ_r is the relative permittivity of the dielectric, and the μ_r is the relative permeability of the dielectric. With a larger ϵ_r, the wavelength at a specific frequency is smaller. Because of the smaller wavelength, the notch comes earlier and the BR peak width becomes narrower. The notch shifts by ∼50 MHz and the channel gain at the notch may vary by -5 ∼ 7 dB. The table first hurts the transmission and then the channel gain with the table goes over the one without the table with the frequency going up. Moreover, when the relative permittivity of the table is lowered from 8.13 to 2, the notch is shifted to the right compared with the blue curve showing the results with the $\epsilon_r = 8.13$ table, as shown by the yellow curve in Figs. 2 (b), (c), (d), but it is still on the left of the notch of the red curve showing the results when the arms are floating in the air ($\epsilon_r = 1$) by 10 ∼ 20 MHz.

III. Experiment Setup and Procedure

Following the conclusions obtained from the simulations, the experiments with a wearable transmitter and receiver, a table in the meeting room environment, and wristbands, as shown in Fig. 3, are implemented. This section specifically describes

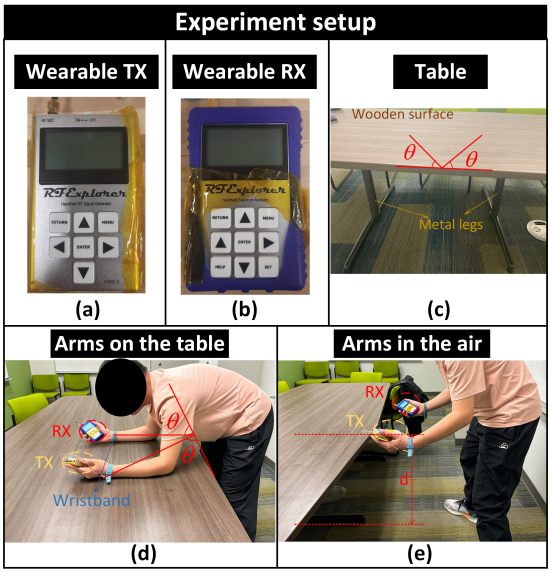

Fig. 3: Experiment setup. (a) RF Explorer signal generator as TX. (b) RF Explorer spectrum analyzer as RX. (c) Experiment table with a wooden surface and metal legs. (d) Experiment scenario when arms are on the table. (e) Experiment scenario when the arms are in the air.

each of them used in the experiment, the calibration of the wearable devices as well as the experiment procedure.

A. Experiment Setup

1) Wearable TRx: The handheld RF Explorer signal generator (RFE6GRN) is used as the transmitter. It can support a frequency range of 24 MHz $\sim$ 6 GHz with a step of 1 kHz and frequency stability of 0.5 ppm, offering the output power of -40 dBm $\sim$ -30 dBm and -10 dBm $\sim$ 0 dBm with a step of 3 dB. The power level 3 (around -1 dBm) with $\sim$0.8 V peak-to-peak voltage is used, which satisfies the safety limits from the International Commission on Non-ionizing Radiation Protection (ICNIRP). The output impedance of this device is 50 Ω.

The handheld RF Explorer spectrum analyzer (WSUB1G+) is used as a receiver. It covers the frequency from 50 kHz to 960 MHz with a frequency resolution of 1 kHz, an amplitude resolution of 0.5 dBm, and a dynamic range of -125 dBm to 10 dBm. The frequency stability is $\pm$10 ppm, and the amplitude stability is $\pm$2 dBm. It has an input impedance of 50 Ω. Though the prior arts [6] on wide-band body channel characterization used high impedance capacitive termination that is proven to be significantly beneficial in EQS, to keep the variability apart from the choice of receiver termination, this paper depicts the measurements without the buffer. Both transmitter and receiver have grounded metallic cases so the contact between the human body and the metallic cases is prevented by using a layer of foam to isolate them. Long SMA cables are prevented to avoid the excessive radiation between the cables leading to over-optimistic measured channel gain.

2) Calibration: The wearable devices, RF Explorer signal generator and spectrum analyzer need to be calibrated for the experiment. To calibrate them, the RF explorer signal generator is connected to the benchtop Keysight spectrum analyzer with an SMA cable. At the fixed power level, the frequency is changed from 30 MHz to 300 MHz with a step of 10 MHz, and the power shown on the benchtop spectrum analyzer is recorded as the calibrated transmitted power from the RF Explorer signal generator, denoted as $\mathrm{P_{trans}}$. Similarly, for the calibration of the receiver, the RF Explorer spectrum analyzer is connected to a bench Keysight signal generator. At each test frequency, the power is swept from -25 dBm to -85 dBm where the received power lies, with a step of -10 dBm. The difference between the output power from the benchtop Keysight signal generator and the power shown by the RF Explorer spectrum analyzer is denoted as a correction factor c. Therefore, assuming the received power is $\mathrm{P_{rx}}$ the channel gain is calculated by $\mathrm{P_{rx}} - \mathrm{P_{trans}} - \mathrm{c}$.

B. Experiment Procedure

Fig. 4 (a) shows the experiment when the arms are placed on the table. The angles are converted to the distances between the transmitter and the receiver based on the trigonometric function and the length of the arms placed on the table. The distance between the transmitter and receiver decreases when the angle goes larger. Fig. 4 (b) shows the experiment scenario when the arms are in the air. The height of the arms and devices is kept the same to keep similar parasitic coupling between the human body and surroundings [2]. For both experiments, at each angle, the frequency is swept from 30 MHz to 300 MHz with a step of 10 MHz, and each reading is repeatedly recorded three times.

IV. Experiment Results

Figs. 4 shows the experiment results. The average value of the three readings is used to plot the curves while the error bars show the obtained minimum and maximum values at each point. At 50 degrees and 65 degrees, the table makes a limited difference below around 120 MHz because before the body resonance peak, the transmitter dipole radiates in the electrostatic region and the wave does not propagate through the medium. Moreover, the distance between the transmitter and the receiver does not have much influence on the frequency of the body resonance peak since it is still well below the wavelength. When the frequency exceeds 120 MHz, an apparent notch shift of 100 MHz and 77 MHz can be observed so that the table can hurt the transmission before the crossing point and help the transmission after that. The table can hurt the transmission by up to 10 dB at 50 degrees and 17 dB at 65 degrees. Moreover, it can help the transmission by 20 dB and 14 dB correspondingly. However, at 80 degrees, since the distance between the transmitter and the receiver is too close to each other, the inter-device coupling plays a dominant role and the receiver is completely within the near-field region. Therefore, the table does not make much difference in the channel characteristics or lead to an apparent notch shift, but it boosts the transmission over all frequencies by up to 6 dB.

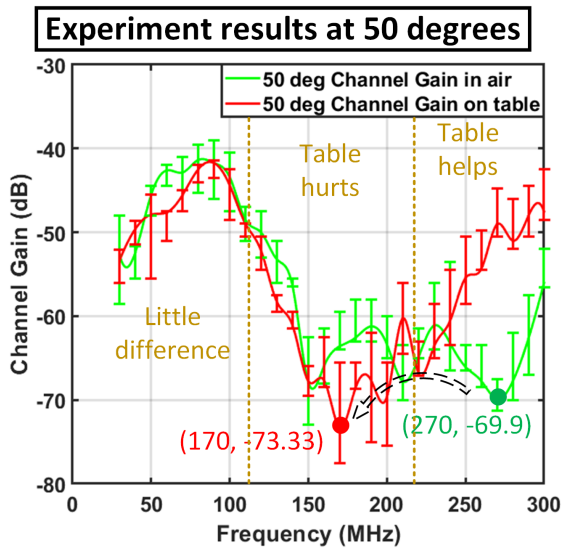

(a) 50 degrees experiment results

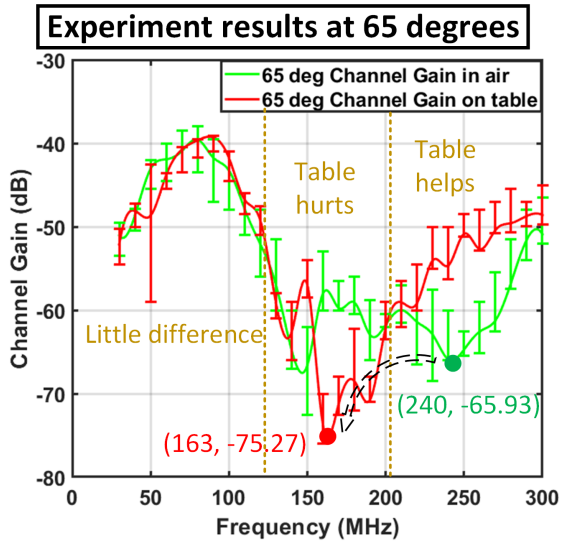

(b) 65 degrees experiment results

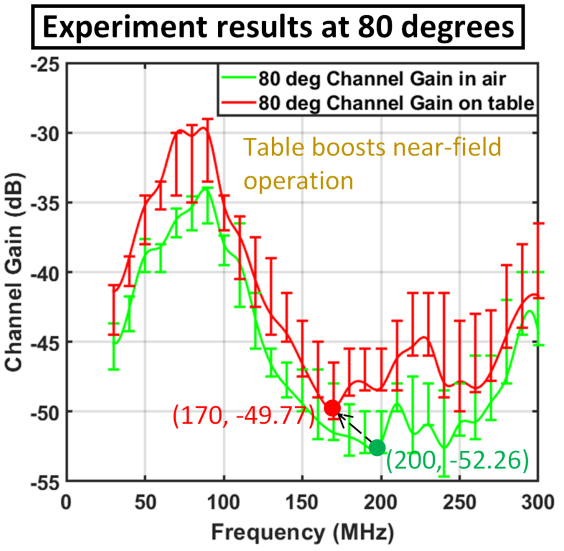

(c) 80 degrees experiment results

Fig. 4: Experiment results. The green curve shows the results when the arms float in the air, and the red curve shows the results when the arms are placed on the table. (a) Experiment results at 50 degrees; (b) Experiment results at 65 degrees; (c) Experiment results at 80 degrees

V. Conclusion

In conclusion, the influence of a table as an external object on the channel characteristics of HBC in the BR region is presented in this work. Firstly, it can be observed from the simulation that the table can shift the notch to a lower frequency because of the participation of the dielectric with a higher permittivity leading to a smaller wavelength. Higher permittivity leads to a more leftward notch. Then the experiments with the same setup as the simulation are implemented with the frequency sweeping from 30 MHz to 300 MHz with a step of 10 MHz. The results show that at 50 and 65 degrees, the table makes an apparent notch shift by up to 100 MHz after around 120 MHz and channel gain change by -17∼20 dB. Before that, it does not make much difference, which is applicable for stable high-speed communication. Moreover, at 80 degrees, the table does not make an apparent difference because of the inter-device coupling which plays a dominant role. The variability in notch position with the change in the termination impedance via the inclusion of a buffer at the receiver can be studied in the future. More detailed study on the influence of external objects on BR HBC channel gain will be conducted in the future, such as the scenarios of different types of table tops, sitting on a wooden stool, standing with bare feet or one foot lifted, different distances between the arm and the table, etc.

Acknowledgement

This work was supported by Quasistatics, Inc. under the Grant 40003567.

References

[1] Lucev, I. Krois, and M. Cifrek, "A capacitive intrabody communication channel from 100 khz to 100 mhz," *IEEE Transactions on Instrumentation and Measurement*, vol. 61, no. 12, pp. 3280–3289, 2012.

[2] S. Maity, M. He, M. Nath, D. Das, B. Chatterjee, and S. Sen, "Bio-physical modeling, characterization, and optimization of electro-quasistatic human body communication," *IEEE Transactions on Biomedical Engineering*, vol. 66, no. 6, pp. 1791–1802, 2019.

[3] D. Yang, S. Maity, and S. Sen, "Physically secure wearable–wearable through-body interhuman body communication," *Frontiers in Electronics*, vol. 2, p. 807051, 2022.

[4] S. Sarkar, A. Datta, M. Nath, D. Yang, S. Maity, and S. Sen, "Electro-quasistatic human-structure coupling for human presence detection and secure data offloading," in *2023 45th Annual International Conference of the IEEE Engineering in Medicine & Biology Society (EMBC)*, 2023, pp. 1–4.

[5] J. Park, H. Garudadri, and P. P. Mercier, "Channel modeling of miniaturized battery-powered capacitive human body communication systems," *IEEE Transactions on Biomedical Engineering*, vol. 64, no. 2, pp. 452–462, 2017.

[6] S. Avlani, M. Nath, S. Maity, and S. Sen, "A 100khz-1ghz termination-dependent human body communication channel measurement using miniaturized wearable devices," in *2020 Design, Automation & Test in Europe Conference & Exhibition (DATE)*, 2020, pp. 650–653.

[7] B. Kibret, A. K. Teshome, and D. T. H. Lai, "Characterizing the human body as a monopole antenna," *IEEE Transactions on Antennas and Propagation*, vol. 63, no. 10, pp. 4384–4392, 2015.

[8] S. Gabriel, R. W. Lau, and C. Gabriel, "The dielectric properties of biological tissues: Ii. measurements in the frequency range 10 hz to 20 ghz," *Physics in Medicine & Biology*, vol. 41, no. 11, p. 2251, nov 1996. [Online]. Available: https://dx.doi.org/10.1088/0031-9155/41/11/002

[9] "NEVA Electromagnetics LLC — VHP-Female model v2.2 - VHP-Female College," https://www.nevaelectromagnetics.com/vhp-female-2-2, [accessed August 27, 2020].

[10] S. Maity, M. Nath, G. Bhattacharya, B. Chatterjee, and S. Sen, "On the safety of human body communication," *IEEE Transactions on Biomedical Engineering*, vol. 67, no. 12, pp. 3392–3402, 2020.